Direct simulation Monte Carlo method for the Uehling-Uhlenbeck-Boltzmann equation

Alejandro L. Garcia*
Institute for Scientific Computing Research, LLNL, Livermore, California 94551, USA

Wolfgang Wagner
Weierstrass Institute for Applied Analysis and Stochastics, Berlin, Germany

(Received 26 August 2002; revised manuscript received 31 July 2003; published 13 November 2003)

In this paper we describe a direct simulation Monte Carlo algorithm for the Uehling-Uhlenbeck-Boltzmann equation in terms of Markov processes. This provides a unifying framework for both the classical Boltzmann case as well as the Fermi-Dirac and Bose-Einstein cases. We establish the foundation of the algorithm by demonstrating its link to the kinetic equation. By numerical experiments we study its sensitivity to the number of simulation particles and to the discretization of the velocity space, when approximating the steady-state distribution.

DOI: 10.1103/PhysRevE.68.056703 PACS number(s): 02.70.Rr, 51.10.+y

I. INTRODUCTION

The recent landmark experiments of Bose-Einstein condensation have generated significant interest in quantum ideal gases (see Ref. [1], and references therein). Kinetic theory is useful in the study of a quantum gas, especially when the particle dynamics can be decomposed into two-body collisions and a mean field potential. For this regime, Uehling and Uhlenbeck [2] extended the Boltzmann equation to quantum systems by including the Pauli factor. In the spatially homogeneous case, this equation takes the form

$$\frac{\partial}{\partial t}f(t,v)=\int_{\mathbb{R}^3}dw\int_{\mathcal{S}^2}de\,B(v,w,e)\{[1+\theta f(t,v)]\times[1+\theta f(t,w)]f(t,v^*)f(t,w^*)-[1+\theta f(t,v^*)]\times[1+\theta f(t,w^*)]f(t,v)f(t,w)\},\qquad(1.1)$$

with initial condition $f(0,v)=f_0(v)$. The postcollision velocities corresponding to $v,w\in\mathbb{R}^3$ are

$$v^*(v,w,e)=v+e(e,w-v),$$

$$w^*(v,w,e)=w-e(e,w-v),\quad e\in\mathcal{S}^2,\qquad(1.2)$$

where $\mathcal{S}^2\subset\mathbb{R}^3$ is the unit sphere and $(.,.)$ denotes the scalar product in the Euclidean space $\mathbb{R}^3$. The function B is the collision kernel, which, in case of hard sphere molecules, takes the form $B(v,w,e)=\text{const}\times|(e,w-v)|$. Note that $n=\int_{\mathbb{R}^3}f_0(v)\,dv$ is the average number of physical particles per unit volume in position space. Equation (1.1) includes (namely, for $\theta=0$) the Boltzmann equation of classical statistics as a special case. It differs from the latter in the case of Bose-Einstein statistics ($\theta=+1$) and in the case of Fermi-Dirac statistics ($\theta=-1$). The case $\theta=+1$ has been considered recently in Ref. [3]. The kinetics of quantum systems in the mean field approximation has been extensively studied in the literature. We refer to Ref. [4] for a general discussion on the nonlinearities originated from the quantum nature of the particles in Boltzmann-like evolution equations.

Direct simulation Monte Carlo (DSMC) has been the most widely used numerical algorithm for the classical Boltzmann equation [5]. Stochastic particle algorithms for the Uehling-Uhlenbeck-Boltzmann (UUB) equation were first developed to simulate the Fermi-Dirac dynamics of nucleons during heavy ion collisions [6–8]. These numerical methods were later reformulated into a DSMC-based framework by Lang *et al.* [9]. Similar Monte Carlo algorithms have been used to study the dynamics of cooling [10] and trapping [11] in Bose-Einstein condensation. These quantum kinetic computations have been combined with numerical solutions of the generalized Gross-Pitaevskii equation to model the thermal cloud and its interaction with the condensate wave function at a finite temperature [12,13]. Dense gas corrections to the UUB equation have been modeled using the consistent Boltzmann algorithm [14], a dense gas variant of DSMC. This algorithm has been used to include virial corrections to UUB simulations [15,16]. Its asymptotic properties in the Boltzmann case have been studied in Ref. [17].

In this paper we describe a DSMC algorithm for the Uehling-Uhlenbeck-Boltzmann equation in terms of Markov processes. This provides a unifying framework for both the classical Boltzmann case as well as the Fermi-Dirac and Bose-Einstein cases. We establish the foundation of the algorithm by demonstrating its link to Eq. (1.1). Using numerical experiments we study its sensitivity to the number of simulation particles and to the discretization of the velocity space, when approximating the steady-state distribution.

The paper is organized as follows. In Sec. II we give a detailed description of the DSMC algorithm starting from a corresponding Markov jump process. Section III provides a heuristic derivation of the limiting equation when the number of simulation particles tends to infinity. In Sec. IV we study the equilibrium behavior of the solution to the UUB equation. Finally, Sec. V contains results of numerical experiments. We calculate approximations to the equilibrium

*Permanent address: Department of Physics, San Jose State University, San Jose, CA, USA.

solution using the particle algorithm. We study the error depending on the numerical parameters such as particle number or number of cells in the velocity space.

II. DESCRIPTION OF THE ALGORITHM

We introduce a Markov process

$$Z(t)=(V_1(t),\ldots,V_N(t)),\quad t\geqslant 0, \tag{2.1}$$

defined by the infinitesimal generator

$$\mathcal{A}(\Phi)(z)=\frac{n}{2N}\sum_{1\leqslant i\neq j\leqslant N}\int_{\mathcal{S}^2}Q(z,i,j,e)\times\{\Phi[J(z,i,j,e)]-\Phi(z)\}de, \tag{2.2}$$

where

$$z=(v_1,\ldots,v_N)\in(\mathbb{R}^3)^N=\mathcal{Z} \tag{2.3}$$

and N is the number of simulation particles. The jump transformation is [cf. Eq. (1.2)]

$$[J(z,i,j,e)]_k=\begin{cases} v_k & \text{if} \quad k\neq i,j \\ v^*(v_i,v_j,e) & \text{if} \quad k=i \\ w^*(v_i,v_j,e) & \text{if} \quad k=j. \end{cases} \tag{2.4}$$

The intensity function has the form

$$Q(z,i,j,e)=Y\left(\frac{n}{N}\sum_{k=1}^{N}g(v^*(v_i,v_j,e),v_k),\times\frac{n}{N}\sum_{k=1}^{N}g(w^*(v_i,v_j,e),v_k)\right)B(v_i,v_j,e), \tag{2.5}$$

where g is some mollifying kernel,

$$g(v,w)=g(w,v)\geqslant 0,\quad \int_{\mathbb{R}^3}g(v,w)dw=1, \tag{2.6}$$

intended for approximating Dirac's δ-function. The concrete form of g as well as of the non-negative function Y will be specified later.

For numerical purposes, we rewrite generator (2.2) in the form

$$\mathcal{A}(\Phi)(z)=\int_{\mathcal{Z}}[\Phi(\bar{z})-\Phi(z)]\hat{\mathcal{Q}}(z,d\bar{z}),$$

where

$$\hat{\mathcal{Q}}(z,d\bar{z})=\frac{n}{2N}\sum_{1\leqslant i\neq j\leqslant N}\int_{\mathcal{S}^2}\{\delta_{J(z,i,j,e)}(d\bar{z})Q(z,i,j,e)+\delta_z(d\bar{z})[\hat{Y}(z)\hat{B}(z)-Q(z,i,j,e)]\}de \tag{2.7}$$

and δ denotes the Dirac measure. The functions $\hat{B}$ and $\hat{Y}$ are such that [cf. Eq. (2.5)]

$$Y\left(\frac{n}{N}\sum_{k=1}^{N}g(v^*(v_i,v_j,e),v_k),\frac{n}{N}\sum_{k=1}^{N}g(w^*(v_i,v_j,e),v_k)\right)\leqslant\hat{Y}(z)\quad\forall\ z\in\mathcal{Z} \tag{2.8}$$

and

$$B(v_i,v_j,e)\leqslant\hat{B}(z)\quad\forall\ 1\leqslant i\neq j\leqslant N,\ e\in\mathcal{S}^2,\quad z\in\mathcal{Z}. \tag{2.9}$$

Thus, the pathwise behavior of the process is as follows. Coming to a state (2.3), the process stays there for a random waiting time, which has an exponential distribution with the parameter [cf. Eq. (2.7)]

$$\hat{\pi}(z)=\hat{\mathcal{Q}}(z,\mathcal{Z})=2\pi n\,\hat{Y}(z)\hat{B}(z)(N-1). \tag{2.10}$$

Then the process jumps into a state $\bar{z}$, which is distributed according to the jump distribution

$$\hat{\pi}(z)^{-1}\hat{\mathcal{Q}}(z,d\bar{z})=\frac{1}{N(N-1)}\sum_{1\leqslant i\neq j\leqslant N}\frac{1}{4\pi}\int_{\mathcal{S}^2}\left\{\delta_{J(z,i,j,e)}(d\bar{z})\frac{Q(z,i,j,e)}{\hat{Y}(z)\hat{B}(z)}+\delta_z(d\bar{z})\left[1-\frac{Q(z,i,j,e)}{\hat{Y}(z)\hat{B}(z)}\right]\right\}.$$

Consequently, first the parameters i, j, and e are generated uniformly. Given i, j and e, the jump is fictitious, i.e., the new state is $\bar{z}=z$, with probability

$$1-\frac{Q(z,i,j,e)}{\hat{Y}(z)\hat{B}(z)}. \tag{2.11}$$

Otherwise, the new state is $\bar{z}=J(z,i,j,e)$.

For calculating quantity (2.11), one needs to evaluate the empirical density [cf. Eq. (2.5)]

$$\hat{f}(z,v)=\frac{n}{N}\sum_{k=1}^{N}g(v,v_k), \tag{2.12}$$

for $v=v^*(v_i,v_j,e)$ and $v=w^*(v_i,v_j,e)$. Note that Eq. (2.6) implies

$$\int_{\mathbb{R}^3} \hat{f}(z,v)\,dv = n \quad \forall\ z \in \mathcal{Z}.$$

For numerical purposes, it is convenient to introduce some partition $\mathcal{V}_l, l=1,\ldots,M$, of the velocity space and to use the function

$$g(v,w) = \sum_{l=1}^{M} \frac{1}{|\mathcal{V}_l|} \chi_{\mathcal{V}_l}(v)\chi_{\mathcal{V}_l}(w), \tag{2.13}$$

where χ denotes the indicator function. Let $N_l, l=1,\ldots,M$, be the number of particles with velocities in cell $\mathcal{V}_l$. Then the empirical density (2.12) takes the form

$$\hat{f}(z,v) = \frac{n\,N_{l(v)}}{N|\mathcal{V}_{l(v)}|}, \quad v \in \mathbb{R}^3, \tag{2.14}$$

where $l(v)$ denotes the number of the cell to which v belongs. Note that function (2.14) is constant in each cell.

The following algorithm is obtained.

(a) Generate the initial state z so that Eq. (2.12) approximates f_0 for large N.

(b) Given z calculate the time step

$$\frac{1}{2\pi n\,\hat{Y}(z)\hat{B}(z)(N-1)}$$

according to Eq. (2.10).

(c) Generate i,j,e uniformly and calculate

$$v_i^* = v^*(v_i,v_j,e), \quad v_j^* = w^*(v_i,v_j,e)$$

according to Eq. (2.4).

(d) With probability (2.11), i.e., if

$$\frac{Y(\hat{f}(z,v_i^*),\hat{f}(z,v_j^*))}{\hat{Y}(z)}\,\frac{B(v_i,v_j,e)}{\hat{B}(z)} \leqslant \mathrm{RAND},$$

go to 1.

(e) Replace v_i, v_j by v_i^*, v_j^*.

(f) Update $\hat{B}, \hat{f}, \hat{Y}$ and go to 1.

Some remarks: First, in the Boltzmann case $Y \equiv 1$, the procedure differs slightly from standard DSMC. This is due to the fact that, in general, Y depends on e so that this parameter also must be generated before the rejection. Second, note that the function $\hat{Y}$ in Eq. (2.8) can be adapted during the process of computation, similar to the adaption of the function $\hat{B}$ in Eq. (2.9) depending on the maximum relative velocity. Third, even if $M=\infty$, sum (2.13) remains finite. Alternatively, one considers the set outside some (big) ball in the velocity space as the last cell. The empirical density is there approximated by zero. Finally, the limiting equation (as $N\to\infty$) for this Markov process is the UUB equation (1.1), for the choice

$$Y(x,y) = (1+\theta x)(1+\theta y), \quad x,y \in \mathcal{R}. \tag{2.15}$$

The derivation of this result is presented in the following section.

III. DERIVATION OF THE LIMITING EQUATION

The Markov process (2.1) satisfies

$$\Phi(Z(t)) = \Phi(Z(0)) + \int_0^t \mathcal{A}(\Phi)[Z(s)]\,ds + M(t), \quad t \geqslant 0, \tag{3.1}$$

where $M(t)$ is some martingale term. We consider [cf. Eq. (2.3)]

$$\Phi(z) = \frac{n}{N}\sum_{i=1}^{N} \varphi(v_i), \quad z \in \mathcal{Z},$$

for appropriate test functions φ. Note that

$$\Phi(Z(t)) = \frac{n}{N}\sum_{i=1}^{N} \varphi(V_i(t)) =: \int_{\mathbb{R}^3} \varphi(v)\,\nu^{(N)}(t,dv), \tag{3.2}$$

where $\nu^{(N)}$ is the empirical measure of the particle system (2.1). According to Eqs. (2.2)–(2.5), one obtains

$$\begin{aligned}\mathcal{A}(\Phi)(z) = \frac{n^2}{2N^2} \sum_{1\leqslant i\neq j\leqslant N} \int_{\mathcal{S}^2} Y\Bigg(&\frac{n}{N}\sum_{k=1}^{N} g(v^*(v_i,v_j,e),v_k),\\ &\frac{n}{N}\sum_{k=1}^{N} g(w^*(v_i,v_j,e),v_k)\Bigg)\\ &\times B(v_i,v_j,e)[\varphi(v^*(v_i,v_j,e))\\ &+ \varphi(w^*(v_i,v_j,e)) - \varphi(v_i) - \varphi(v_j)]\,de\end{aligned}$$

and

$$\begin{aligned}\mathcal{A}(\Phi)[Z(s)] = \frac{1}{2}\int_{\mathbb{R}^3}\int_{\mathbb{R}^3}\int_{\mathcal{S}^2} Y\Bigg(&\int_{\mathbb{R}^3} g(v^*,u)\,\nu^{(N)}(s,du),\\ &\int_{\mathbb{R}^3} g(w^*,u)\,\nu^{(N)}(s,du)\Bigg)\\ &\times B(v,w,e)[\varphi(v^*)+\varphi(w^*)\\ &-\varphi(v)-\varphi(w)]\,de\,\nu^{(N)}(s,dv)\,\nu^{(N)}(s,dw)\\ &+ O(N^{-1}),\end{aligned} \tag{3.3}$$

where the functions v^*, w^* depend on the arguments v,w,e as defined in Eq. (1.2).

Suppose that the following relations are fulfilled as $N\to\infty$:

$$\nu^{(N)}(t) \to F(t), \quad M^{(N)}(t) \to 0 \quad \forall\ t \geqslant 0,$$

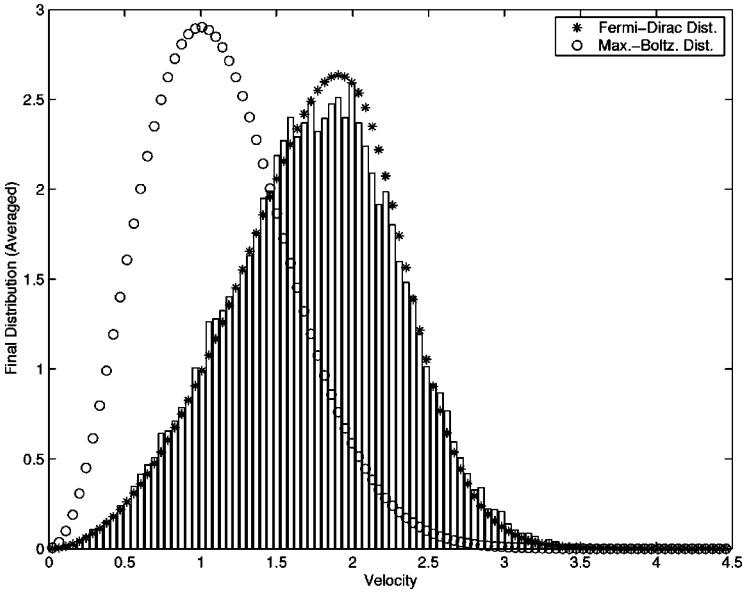

FIG. 1. Steady-state speed distribution in a Fermi-Dirac gas. Data from a simulation with $N=10^4$ particles and $M=10^4$ cells are shown as histogram bars; expected distribution shown by asterisks. The Maxwell-Boltzmann distribution for a gas with the same kinetic energy is shown by open circles for comparison.

for some deterministic measure-valued function $F(t)$. Under certain assumptions concerning this convergence, one can conclude from Eq. (3.1) and (3.3) that the limit $F(t)$ satisfies the equation

$$\begin{aligned}\int_{\mathbb{R}^3}\varphi(v)\,F(t,dv)&\\ =\int_{\mathbb{R}^3}\varphi(v)\,F_0(dv)&\\ +\frac{1}{2}\int_0^t\int_{\mathbb{R}^3}\int_{\mathbb{R}^3}\int_{\mathcal{S}^2}Y\Big(\int_{\mathbb{R}^3}g(v^*,u)F(s,du),&\\ \int_{\mathbb{R}^3}g(w^*,u)F(s,du)\Big)&\\ \times B(v,w,e)[\varphi(v^*)+\varphi(w^*)-\varphi(v)-\varphi(w)]de&\\ \times F(s,dv)F(s,dw)ds.&\end{aligned}$$

The differential form with respect to t is

$$\begin{aligned}\frac{d}{dt}\int_{\mathbb{R}^3}\varphi(v)F(t,dv)=\frac{1}{2}\int_{\mathbb{R}^3}\int_{\mathbb{R}^3}\int_{\mathcal{S}^2}\beta(t,v^*,w^*)B(v,w,e)&\\ \times[\varphi(v^*)+\varphi(w^*)-\varphi(v)-\varphi(w)]de&\\ \times F(t,dv)F(t,dw),&\end{aligned}\tag{3.4}$$

with the initial condition

$$F_0=\lim_{N\to\infty}\nu^{(N)}(0),\tag{3.5}$$

where we denote

$$\beta(t,x,y)=Y\Big(\int_{\mathbb{R}^3}g(x,u)F(t,du),\int_{\mathbb{R}^3}g(y,u)F(t,du)\Big).\tag{3.6}$$

Note that, in case of Eq. (2.13),

$$\int_{\mathbb{R}^3}g(v,u)F(t,du)=\frac{1}{|\mathcal{V}_{l(v)}|}F(t,\mathcal{V}_{l(v)})\quad\forall\ v\in\mathbb{R}^3,$$

and that Eq. (3.5) implies [cf. Eq. (3.2)]

$$F_0(\mathbb{R}^3)=\lim_{N\to\infty}\nu^{(N)}(0,\mathbb{R}^3)=n.$$

Note that the conservation properties are derived from Eq. (3.4), as in the Boltzmann case $Y\equiv 1$, for $\varphi=1,v,\|v\|^2$.

Assume the limiting measures have densities

$$F(t,dv)=f(t,v)dv,$$

the function Y is symmetric, and

$$B(v,w,e)=B(v^*,w^*,e)=B(w,v,e)=B(v,w,-e).\tag{3.7}$$

Note that the hard sphere kernel satisfies (3.7). Applying the substitution $(v^*,w^*)\to(v,w)$, the terms at the right-hand side of Eq. (3.4) transform according to

$$\begin{aligned}\int_{\mathbb{R}^3}\int_{\mathbb{R}^3}\int_{\mathcal{S}^2}\beta(t,v^*,w^*)B(v,w,e)\varphi(v^*)&\\ \times f(t,v)f(t,w)de\,dv\,dw&\\ =\int_{\mathbb{R}^3}\int_{\mathbb{R}^3}\int_{\mathcal{S}^2}\beta(t,v,w)B(v,w,e)\varphi(v)f(t,v^*)&\\ \times f(t,w^*)de\,dv\,dw.&\end{aligned}$$

Removing the test functions, one obtains

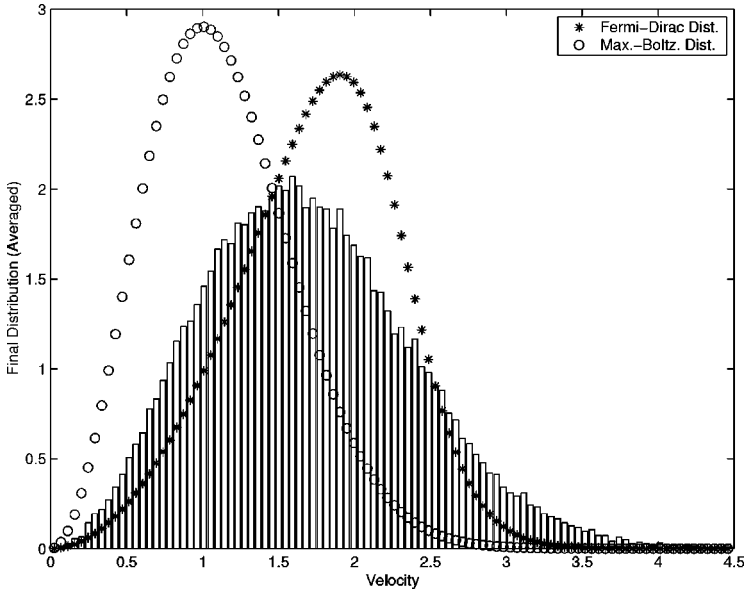

FIG. 2. Same as Fig. 1 but for a simulation with $M=10^6$ velocity cells.

$$\frac{\partial}{\partial t}f(t,v)=\int_{\mathbb{R}^3}dw\int_{S^2}de\,B(v,w,e)\times[\beta(t,v,w)f(t,v^*)f(t,w^*)-\beta(t,v^*,w^*)f(t,v)f(t,w)]. \quad (3.8)$$

$$\frac{\partial}{\partial t}f(t,v)=\int_{\mathbb{R}^3}dw\int_{S^2}de\,B(v,w,e)\times[Y(f(t,v),f(t,w))f(t,v^*)f(t,w^*)-Y(f(t,v^*),f(t,w^*))f(t,v)f(t,w)]. \quad (3.9)$$

If

$$g(x,y)=g^{(N)}(x,y)\to\delta(x-y) \quad \text{as} \quad N\to\infty,$$

then [cf. Eq. (3.6)] $\beta(t,x,y)=Y(f(t,x),f(t,y))$, and Eq. (3.8) takes the form

Equation (1.1) is obtained from Eq. (3.9) for choice (2.15), with the particular cases $\theta=1$ (Bose-Einstein), $\theta=0$ (Boltzmann), and $\theta=-1$ (Fermi-Dirac). Note that since the function Y should be non-negative, it is more accurate to define Eq. (2.15) for $\theta<0$ as

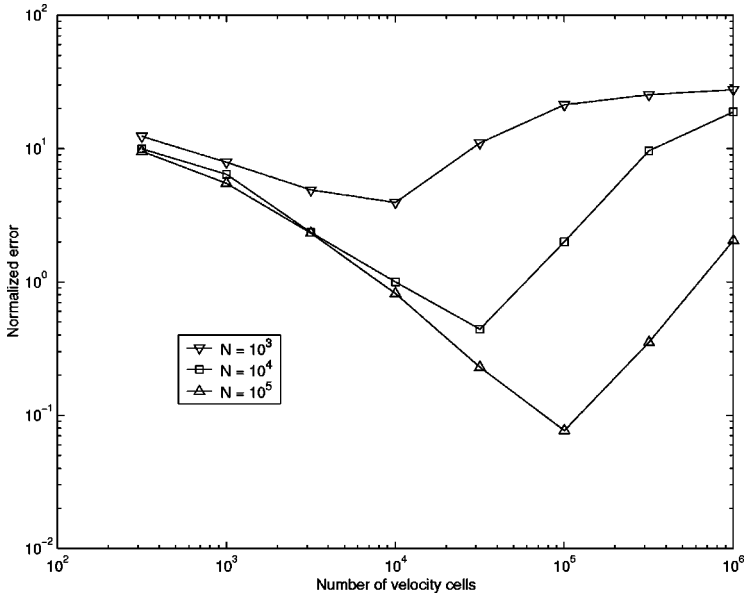

FIG. 3. Normalized error $\overline{E}(N,M)$ in the steady-state Fermi-Dirac speed distribution as a function of the number of velocity cells.

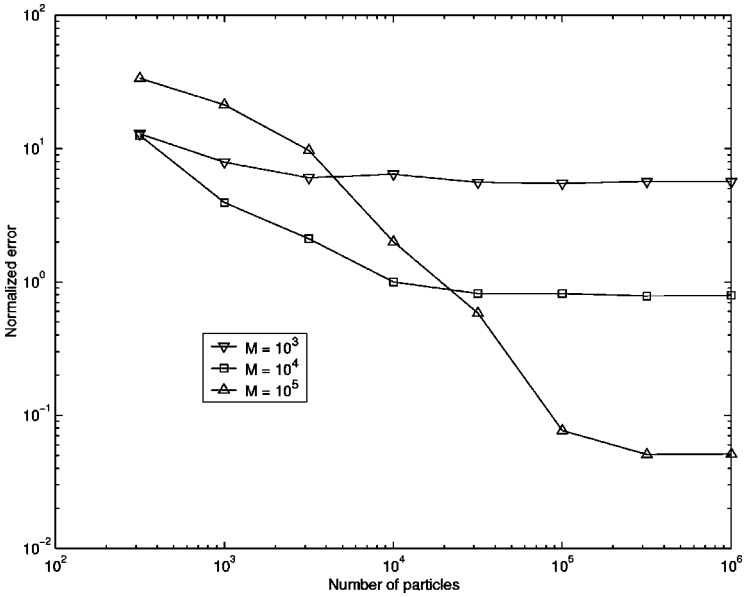

FIG. 4. Normalized error $\bar{E}(N,M)$ in the steady-state Fermi-Dirac speed distribution as a function of the number of particles.

$$Y(x,y)=(1+\theta x)^{+}(1+\theta y)^{+},$$

where $a^{+}=a$ if $a>0$ and $a^{+}=0$ otherwise.

IV. EQUILIBRIUM BEHAVIOR

First we recall the derivation of an H-theorem (cf., e.g., Ref. [18] Sec. 5.4.3). Let f be a solution to Eq. (3.9) with Y as in Eq. (2.15). Defining

$$H(t)=\int_{\mathbb{R}^3}\Big[f(t,v)\ln f(t,v) - \frac{1}{\theta}[1+\theta f(t,v)]\ln[1+\theta f(t,v)]\Big]dv,$$

one obtains

$$\frac{d}{dt}H(t)=\int_{\mathbb{R}^3}\Big[\frac{\partial}{\partial t}f(t,v)\ln f(t,v)+\frac{\partial}{\partial t}f(t,v) - \frac{\partial}{\partial t}f(t,v)\ln[1+\theta f(t,v)]-\frac{\partial}{\partial t}f(t,v)\Big]dv$$
$$=\int_{\mathbb{R}^3}\Big[\frac{\partial}{\partial t}f(t,v)\ln\frac{f(t,v)}{1+\theta f(t,v)}\Big]dv. \tag{4.1}$$

Note that the case $\theta=0$ is easily covered, but in the case $\theta<0$ the condition

$$f(t,v)<-\frac{1}{\theta} \tag{4.2}$$

has to be assumed. Using Eq. (3.9) and the notation $s(t,v)=1+\theta f(t,v)$, the right-hand side of Eq. (4.1) takes the form

$$\int_{\mathbb{R}^3}dv\int_{\mathbb{R}^3}dw\int_{\mathcal{S}^2}de\,B(v,w,e)[s(t,v)s(t,w)f(t,v^*)f(t,w^*)-s(t,v^*)s(t,w^*)f(t,v)f(t,w)]\ln\frac{f(t,v)}{s(t,v)}$$
$$=\int_{\mathbb{R}^3}dv\int_{\mathbb{R}^3}dw\int_{\mathcal{S}^2}de\,B(v,w,e)[s(t,v)\,s(t,w)\,f(t,v^*)\,f(t,w^*)-s(t,v^*)\,s(t,w^*)\,f(t,v)\,f(t,w)]\ln\frac{f(t,w)}{s(t,w)}$$
$$=-\int_{\mathbb{R}^3}dv\int_{\mathbb{R}^3}dw\int_{\mathcal{S}^2}de\,B(v,w,e)[s(t,v)\,s(t,w)\,f(t,v^*)\,f(t,w^*)-s(t,v^*)\,s(t,w^*)\,f(t,v)\,f(t,w)]\ln\frac{f(t,v^*)}{s(t,v^*)}$$
$$=-\int_{\mathbb{R}^3}dv\int_{\mathbb{R}^3}dw\int_{\mathcal{S}^2}de\,B(v,w,e)[s(t,v)\,s(t,w)\,f(t,v^*)\,f(t,w^*)-s(t,v^*)\,s(t,w^*)\,f(t,v)\,f(t,w)]\ln\frac{f(t,w^*)}{s(t,w^*)}$$
$$=\frac{1}{4}\int_{\mathbb{R}^3}dv\int_{\mathbb{R}^3}dw\int_{\mathcal{S}^2}de\,B(v,w,e)[s(t,v)\,s(t,w)\,f(t,v^*)\,f(t,w^*)-s(t,v^*)\,s(t,w^*)\,f(t,v)\,f(t,w)]$$
$$\times\ln\frac{f(t,v)\,f(t,w)\,s(t,v^*)\,s(t,w^*)}{s(t,v)\,s(t,w)\,f(t,v^*)\,f(t,w^*)}. \tag{4.3}$$

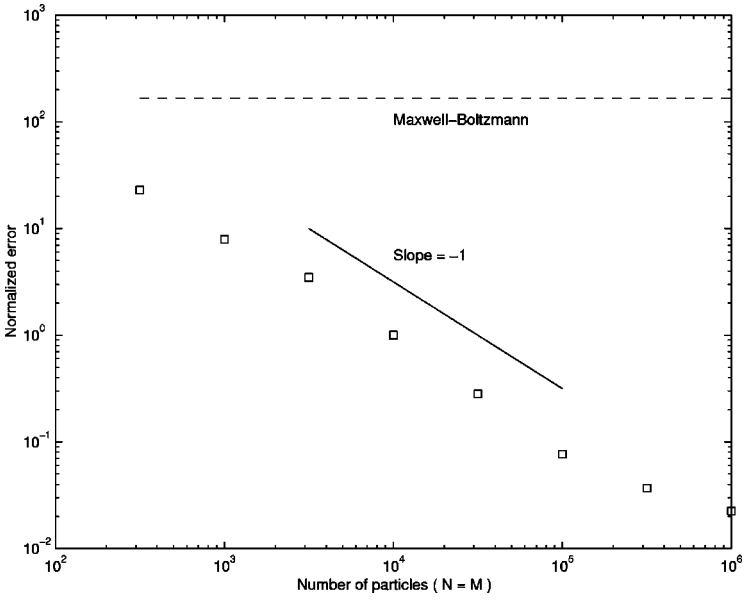

FIG. 5. Normalized error $\overline{E}(N,M)$ in the steady-state Fermi-Dirac speed distribution as a function of $N=M$. For comparison, the error for a Maxwell-Boltzmann distribution (i.e., open circles in Fig. 1) is shown as a dashed line.

From $(b-a)\ln(a/b)\leqslant 0$ and from Eqs. (4.1) and (4.3) one obtains

$$\frac{d}{dt}H(t)\leqslant 0.$$

More details about the derivation of the H theorem can be found in Ref. [4]. The general nonlinear Boltzmann equation considered in this reference, contains as a particular case the Uehling-Uhlenbeck equation (1.1).

Next we consider the problem of the steady state p (cf. Ref. [19] Chap. 17.5]). From Eq. (3.9) one obtains

$$\frac{p(v^*)\,p(w^*)}{Y(p(v^*),p(w^*))}=\frac{p(v)\,p(w)}{Y(p(v),p(w))} \tag{4.4}$$

as a sufficient condition. Assuming

$$Y(x,y)=\tilde{Y}(x)\,\tilde{Y}(y), \tag{4.5}$$

condition (4.4) takes the form

$$\ln\frac{p(v^*)}{\tilde{Y}(p(v^*))}+\ln\frac{p(w^*)}{\tilde{Y}(p(w^*))}=\ln\frac{p(v)}{\tilde{Y}(p(v))}+\ln\frac{p(w)}{\tilde{Y}(p(w))}. \tag{4.6}$$

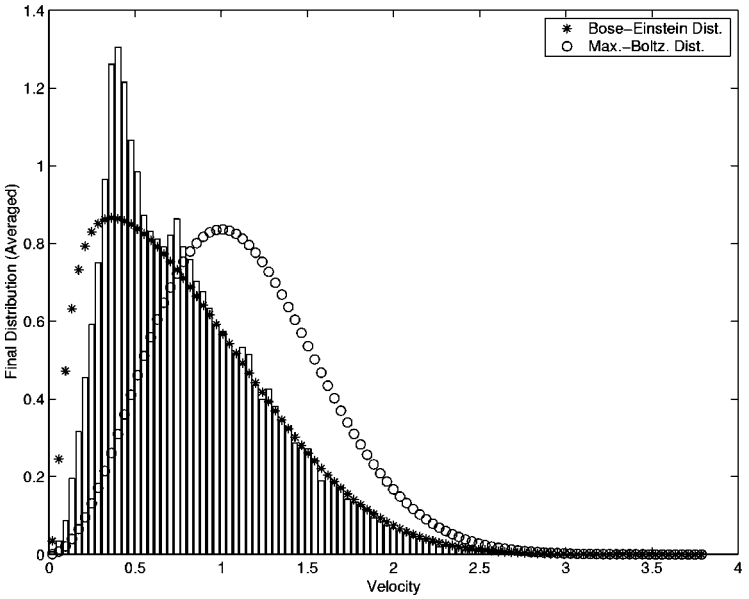

FIG. 6. Steady-state speed distribution in a Bose-Einstein simulation with $N=10^4$ particles and $M=10^4$ cells.

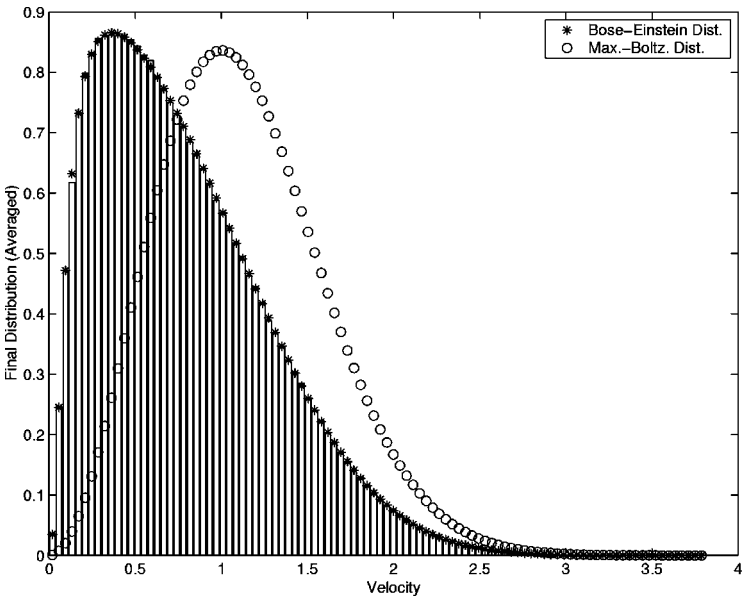

FIG. 7. Steady-state speed distribution in a Bose-Einstein simulation with $N=10^6$ particles and $M=10^6$ cells.

Since $\psi(v^*)+\psi(w^*)=\psi(v)+\psi(w)$ implies $\psi(v)=c_1+c_2\|v-\overline{v}\|^2$, for some $c_1,c_2\in\mathcal{R}$ and $\overline{v}\in\mathbb{R}^3$, we obtain from Eq. (4.6),

$$p(v)=\tilde{Y}(p(v))\exp(c_1+c_2\|v-\overline{v}\|^2). \tag{4.7}$$

Function (2.15) satisfies (4.5), with $\tilde{Y}(x)=1+\theta x$. Thus, Eq. (4.7) implies

$$p(v)=\frac{\exp(c_1+c_2\|v-\overline{v}\|^2)}{1-\theta\exp(c_1+c_2\|v-\overline{v}\|^2)}$$

$$=\frac{1}{\exp(-c_1-c_2\|v-\overline{v}\|^2)-\theta}. \tag{4.8}$$

The parameters c_1, c_2, and $\overline{v}$ have to be chosen to fit the conserved quantities. Necessary conditions (for positivity and integrability) are

$$\exp(-c_1)>\theta, \quad c_2<0. \tag{4.9}$$

Note that, in the case $\theta<0$, condition $p(v)<-1/\theta$ [cf. Eq. (4.2)] is satisfied.

Let $\overline{v}=0$, $c_1=-\ln A$, $c_2=-\alpha$ so that the equilibrium density (4.8) takes the form

$$p(v)=p_{\alpha,A,\theta}(v)=\frac{1}{A\exp(\alpha\|v\|^2)-\theta}, \tag{4.10}$$

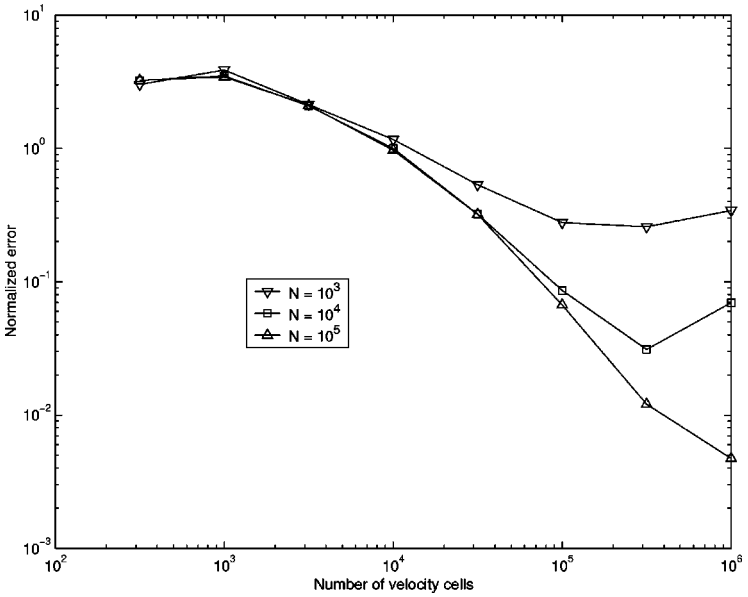

FIG. 8. Normalized error $\overline{E}(N,M)$ in the steady-state Bose-Einstein speed distribution as a function of the number of velocity cells.

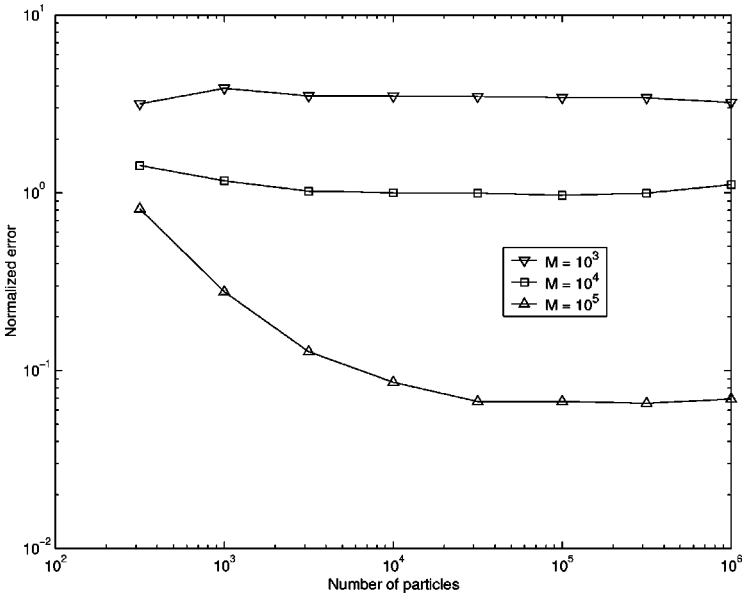

FIG. 9. Normalized error $\bar{E}(N,M)$ in the steady-state Bose-Einstein speed distribution as a function of the number of particles.

where, according to Eq. (4.9),

$$A > \max(\theta,0) \quad \text{and} \quad \alpha > 0. \tag{4.11}$$

Note that, in case $\theta > 0$ and $A \to \theta$, some δ-like distribution is obtained (Bose-Einstein condensation), while in case $\theta < 0$ and $A \to 0$, an approximate uniform distribution is obtained (Fermi level). For $A \to \infty$ distributions in both cases are close to a Maxwellian (with mean $\sim 1/A$). Finally, in case $\theta = 0$, a pure Maxwellian is obtained. In the Fermi-Dirac case $\theta < 0$, the equilibrium density is bounded by $-1/\theta$. If the function $f(t,v)$ exceeds this bound, the gain term in Eq. (3.9) becomes zero so that the function decreases. One might expect that the correct equilibrium density is obtained even for initial densities f_0 that are not bounded by $-1/\theta$.

If the empirical density (2.14) exceeds the bound $-1/\theta$, then no more particles will come to the corresponding cell, but particles can leave that cell. So that, at steady state, the empirical density will satisfy the necessary condition (at least approximately as $N \to \infty$).

V. NUMERICAL EXPERIMENTS

Since the equilibrium density is isotropic, it will be useful to consider the speed distribution defined as

$$\tilde{p}(u) = \frac{4\pi u^2}{A \exp(\alpha u^2) - \theta}, \tag{5.1}$$

where $u = \|v\|$. Note that the speed distribution is merely $p(v)$ given in Eq. (4.10) integrated over angle.

A. Fermi-Dirac case

Figure 1 shows the steady-state speed distribution (5.1) measured in the simulation of a gas of Fermi-Dirac particles ($\theta = -1$). The parameters in this case are $A = 0.01$ and $\alpha = 1$ [cf. (4.11)], which correspond to a temperature of $0.21 T_F$, where T_F is the Fermi temperature [20]. The simulation used $N = 10^4$ particles and $M = 10^4$ velocity cells, which were cubic with a width of $\Delta v = 0.45$.[1] Note that for this choice of parameters we find good agreement with the expected equilibrium distribution.

To quantify this agreement, the square integrated difference between the measured and expected speed distribution was evaluated as

$$E(N,M) = \int_0^\infty [\tilde{p}(u) - \tilde{p}_s(u;N,M)]^2 \, du,$$

where $\tilde{p}_s$ is the estimated steady-state distribution from the simulation. For the results shown in Fig. 1 this error was 0.031. For comparison, a similar simulation for a Maxwell-Boltzmann gas (i.e., standard DSMC) had an integrated square difference of about 10^{-5}. As the value of E also varies with the parameters A and α, we use the normalized error defined as $\bar{E}(N,M) = E(N,M)/E(10^4,10^4)$.

[1] Actually the value of M is rounded to the nearest cubic integer, e.g., for $M = 10^5$ the number of velocity cells is actually $97\,336 = 46^3$.

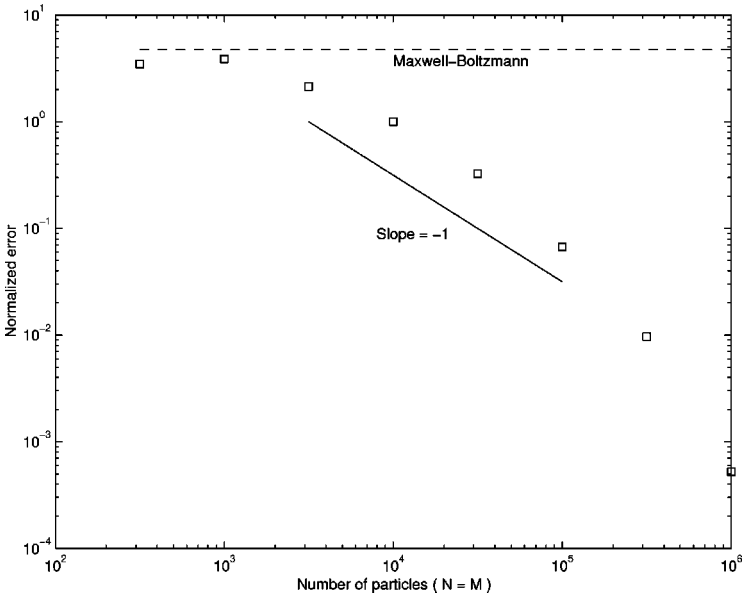

FIG. 10. Normalized error $\overline{E}(N,M)$ in the steady-state Bose-Einstein speed distribution as a function of $N=M$. For comparison, the error for a Maxwell-Boltzmann distribution (i.e., open circles in Fig. 6) is shown as a dashed line.

Interestingly, increasing the number of velocity cells can *reduce* the accuracy of the distribution, as seen in Fig. 2, which is similar to the previous figure but with the number of velocity cells increased to $M=10^6$ (and the cell size reduced to $\Delta v=0.09$). When the number of cells is significantly larger than the number of particles, Fermi exclusion is not accurately modeled.

This effect is confirmed in Fig. 3, which shows the normalized error as a function of the number of cells for various values of N. On the other hand, for a given number of cells the error plateaus when $N \geqslant M$, as shown in Fig. 4. Roughly speaking, the error is minimum when $N \approx M$ and when we take the number of particles equal to the number of cells we find that $\overline{E} \approx 1/M$, as shown in Fig. 5. One also finds that even when $N=M \approx 300$ the distribution retains a strong quantum signature, when compared with the corresponding Maxwell-Boltzmann distribution (dashed line in Fig. 5). Note that all of these results are for simulations using the parameters $A=0.01$ and $\alpha=1$; for different values of the parameters we expect quantitatively different errors (e.g., $\overline{E}$ decreases as A increases) but qualitatively similar dependence on N and M.

B. Bose-Einstein case

Figure 6 shows the steady-state speed distribution (5.1) measured in the simulation of a gas of Bose-Einstein particles ($\theta=1$). The parameters in this case are $A=1.01$ and $\alpha=1$ [cf. Eq. (4.11)], which correspond to a temperature of $1.08T_c$, where T_c is the critical temperature [20]. The simulation parameters are $N=10^4$, $M=10^4$, and $\Delta v=0.38$. Although the agreement with the expected distribution is poor, Fig. 7 shows that the agreement is very good when N and M are increased to 10^6 (and Δv reduced to 0.08).

Figure 8 shows that in these simulations of a Bose-Einstein gas, the normalized error drops with increasing number of particle cells until $M \approx 100N$. On the other hand, for a given number of cells $\overline{E}(N,M)$ is approximately constant in N, as shown in Fig. 9, when $N>M/10$. Finally, graphing $\overline{E}(N,M)$ versus $N=M$ (Fig. 10) shows that the error decreases roughly as $1/M$ except for small simulations ($M<10^3$). For those simulations the error plateaus at approximately that of a DSMC simulation for a Maxwell-Boltzmann gas (i.e., $\theta=0$), though the distribution is *not* Maxwellian. Again, all of the Bose-Einstein simulations used the parameters $A=1.01$ and $\alpha=1$; for different values of the parameters we expect quantitatively different errors (e.g., $\overline{E}$ decreases as A increases) but qualitatively similar dependence on N and M.

VI. CONCLUSION

The purpose of this paper was twofold. In the first part we have described a DSMC algorithm for the Uehling-Uhlenbeck-Boltzmann equation in terms of Markov processes. This approach provided a unifying framework for both the classical Boltzmann case as well as the Fermi-Dirac and Bose-Einstein cases. We have also established the foundation of the algorithm by demonstrating its link to the kinetic equation.

The second part of the paper was devoted to numerical experiments. After recalling some known properties related to the steady-state distribution, we have shown that the algorithm produces correct results both in Fermi-Dirac and Bose-Einstein cases. We have also studied the sensitivity of the algorithm to the number of simulation particles and to the discretization of the velocity space. It turned out that the number of velocity cells must be appropriately adapted to the number of simulation particles in order to obtain convergence.

ACKNOWLEDGMENTS

One of the authors (A.L.G.) wishes to thank the Weierstrass Institute for Applied Analysis and Stochastics, where this research was initiated, for its hospitality during his stay in Berlin. This work was supported, in part, by a grant from the European Commission DG 12 (Grant No. PSS*1045) and was performed, in part, at Lawrence Livermore National Laboratory under the auspices of the U.S. Department of Energy under Contract No. W-7405-Eng-48.

[1] F. Dalfovo, S. Giorgini, L. Pitaevskii, and S. Stringari, Rev. Mod. Phys. **71**, 463 (1999).
[2] E.A. Uehling and G.E. Uhlenbeck, Phys. Rev. **43**, 552 (1933).
[3] X. Lu, J. Stat. Phys. **98**, 1335 (2000).
[4] G. Kaniadakis, Phys. A **296**, 405 (2001).
[5] G.A. Bird, *Molecular Gas Dynamics and the Direct Simulation of Gas Flows* (Clarendon Press, Oxford, 1994).
[6] G.F. Bertsch, H. Kruse, and S. Das Gupta, Phys. Rev. C **29**, 673 (1984); **33**, 1107(E) (1986).
[7] G.F. Bertsch and S. Das Gupta, Phys. Rep. **160**, 189 (1988).
[8] A. Bonasera, F. Gulminelli, and J. Molitoris, Phys. Rep. **243**, 1 (1994).
[9] A. Lang, H. Babovsky, W. Cassing, U. Mosel, H.-G. Reusch, and K. Weber, J. Comput. Phys. **106**, 391 (1993).
[10] H. Wu, E. Arimondo, and C. Foot, Phys. Rev. A **56**, 560 (1997).
[11] E. Cerboneschi, C. Menchini, and E. Arimondo, Phys. Rev. A **62**, 013606 (2000).
[12] B. Jackson and E. Zaremba, Phys. Rev. Lett. **87**, 100404 (2001).
[13] B. Jackson and E. Zaremba, Phys. Rev. A **66**, 033606 (2002).
[14] F.J. Alexander, A.L. Garcia, and B.J. Alder, Phys. Rev. Lett. **74**, 5212 (1995).
[15] G. Kortemeyer, F. Daffin, and W. Bauer, Phys. Lett. B **374**, 25 (1996).
[16] K. Morawetz, V. Spicka, P. Lipavsky, G. Kortemeyer, C. Kuhrts, and R. Nebauer, Phys. Rev. Lett. **82**, 3767 (1999).
[17] A.L. Garcia and W. Wagner, J. Stat. Phys. **101**, 1065 (2000).
[18] R.L. Liboff, *Kinetic Theory: Classical, Quantum, and Relativistic Descriptions*, 2nd ed. (Wiley, New York, 1998).
[19] S. Chapman and T.G. Cowling, *The Mathematical Theory of Non-Uniform Gases. An Account of the Kinetic Theory of Viscosity, Thermal Conduction and Diffusion in Gases* (Cambridge University Press, London, 1970).
[20] K. Huang, *Statistical Mechanics*, 2nd ed. (Wiley, New York, 1987).